Privacy-Preserving and Collision-Free Formation Control for Heterogeneous Multiagent Systems

Jinliang Liu, *Senior Member, IEEE*, Shiming Mao, Lijuan Zha, Engang Tian, *Senior Member, IEEE*, and Chen Peng, *Senior Member, IEEE*

***Abstract*—This article proposes a secure time-varying formation (TVF) control framework for heterogeneous multi-agent systems (HMASs) operating under the threats of communication eavesdropping, non-cooperative dynamic obstacles, and input saturation. The framework integrates cyber-layer and physical-layer components that collaboratively address these challenging conditions. In the cyber-layer, an intermittent privacy-preserving observer is designed, which fuses periodic activation with a threat-based dynamic triggering strategy. This design effectively mitigates eavesdropping risks while resolving the irreversibility dilemma inherent in static masking techniques. At the physical-layer, the controller is formulated as a quadratic programming problem integrating Lyapunov functions and control barrier functions. It ensures the operational safety of high-order heterogeneous agents in environments with obstacles and input saturation. The effectiveness and advantages of the proposed framework are demonstrated through simulations on a heterogeneous system consisting of uncrewed aerial vehicles (UAVs) and uncrewed ground vehicles (UGVs).**

***Index Terms*—Heterogeneous multi-agent systems (HMASs), security control, intelligent intermittent privacy-preserving mechanism.**

I. Introduction

COOPERATIVE control of multi-agent systems has been widely applied in UAV and UGV scenarios, where formation control enables structured collaboration. Early research mainly focused on time-varying formation (TVF) control of homogeneous systems [1], [2], [3]; however, their limited adaptability in complex and high-threat environments has motivated the development of heterogeneous multi-agent systems (HMASs) that exploit agents' complementary capabilities [4], [5], [6]. With enhanced flexibility, robustness, and fault tolerance, HMASs play a crucial role in patrol, search, and rescue tasks [7], [8]. Based on consensus theory [9], HMAS formation control enables agents to maintain geometric configurations while leveraging heterogeneous dynamics to accomplish complex cooperative missions [10], [11], [12]. Despite recent advances [13], [14], [15], effective formation control remains challenging due to mismatched dynamics and state orders. To improve adaptability, TVF control approaches, including multi-layer strategies [16], [17] and output regulation frameworks via internal models [18] have been proposed, enabling HMASs to simultaneously track virtual leaders and reference TVF systems [19].

Ensuring the safety and security of HMASs in complex environments remains a critical challenge, involving communication integrity, cyber resilience, and data privacy [20], [21], [22]. Existing privacy-preserving approaches based on masking functions suffer from inherent trade-offs: vanishing masks degrade control accuracy [23], [24], [25], permanent masks introduce irreversible leakage [26], and intermittent schemes lack real-time threat responsiveness [27]. To overcome these limitations, this article proposes an intelligent privacy-preserving mechanism that combines periodic activation with threat-triggered masking, tightly couples cyber privacy with physical safety indicators to enable adaptive and proactive defense.

Physical safety of multi-agent systems (MASs) during formation is a fundamental prerequisite for complex task success [28], [29]. Key safety concerns include avoiding noncooperative obstacles in uncertain environments. Extensive studies focus on collision-free formation control, with artificial potential field-based methods widely explored [30], [31]. However, prevailing collision avoidance algorithms often insufficiently address input constraint impacts. To ensure MAS safety under dynamic obstacles and input saturation, control policies integrating control Lyapunov functions (CLFs), exponential control barrier functions (ECBFs), and quadratic programming (QP) have been developed [32], [33]. Nonetheless, most contemporary safety control techniques target homogeneous MASs and simplify high-order systems to lower-order models [34], making them inadequate for safe formation control of high-order HMASs [35], [36]. To facilitate efficient HMAS collaboration under multiple constraints, this article presents a novel control framework. The key contributions are threefold:

1) An intelligent intermittent privacy-preserving (IPP) mechanism with periodic and threat-driven activation to balance security and control accuracy;

Received 21 November 2025; revised 6 January 2026 and 25 January 2026; accepted 21 February 2026. Date of publication 24 February 2026; date of current version 2 June 2026. This work was supported in part by the National Natural Science Foundation of China under Grant 62373252 and Grant 62273174. *(Corresponding author: Jinliang Liu.)*

Jinliang Liu and Shiming Mao are with the School of Computer Science, Nanjing University of Information Science and Technology, Nanjing 210044, China (e-mail: liujinliang@vip.163.com; maoshiming0303@163.com).

Lijuan Zha is with the School of Science, Nanjing Forestry University, Nanjing 210037, China (e-mail: zhalijuan@vip.163.com).

Engang Tian is with the School of Optical-Electrical and Computer Engineering, University of Shanghai for Science and Technology, Shanghai 200093, China (e-mail: tianengang@163.com).

Chen Peng is with the School of Mechatronic Engineering and Automation, Department of Automation, Shanghai University, Shanghai 200444, China (e-mail: c.peng@shu.edu.cn).

Digital Object Identifier 10.1109/TCE.2026.3667772

2) A secure controller with internal-model-based augmentation for safe TVF tracking of high-order HMASs under input saturation and obstacle constraints.
3) A dual-layer architecture that explicitly couples cyber-layer privacy with physical-layer safety by using $h(x)$ to trigger privacy protection, simultaneously addressing privacy threats and safety requirements without compromising system physical safety.

Notation: $\mathbb{R}^n$ denotes the n-dimensional real Euclidean space. For agent i, $x_i \in \mathbb{R}^{n_i}$, $u_i \in \mathbb{R}^{m_i}$, and $y_i \in \mathbb{R}^{p_i}$ represent its state, control input, and output, respectively, where the dimensions depend on the agent dynamics. $\mathcal{M}$ denotes the set of all agents, and $\mathcal{O}_i$ is the set of obstacles within the detection range of agent i. η represents the state of the virtual leader, and f_i denotes the state of the ith TVF. $L_f^{r^b} h$ denotes the r^b-th order Lie derivative of function h along vector field f. $\delta_j(t)$ and μ_j denote the intermittent masking signal and its amplitude vector generated by agent j, respectively. z_i is the internal compensation state of agent i, and Φ_i represents the p-copy internal model associated with A_i^ζ.

II. Preliminaries and Problem Formulation

A. System Modeling

Consider a unified HMAS consisting of n agents and a shared virtual leader. The model of the ith agent can be modeled as

$$\begin{cases} \dot{x}_i(t) = A_i x_i(t) + B_i u_i(t), \\ y_i(t) = C_i x_i(t), \end{cases} \tag{1}$$

where $x_i \in \mathbb{R}^{n_i}$, $u_i \in \mathbb{R}^{m_i}$, and $y_i \in \mathbb{R}^p$ represent the i-th agent's state, input, and output variables, respectively. A_i, B_i, and C_i represent the system state, input, and output matrices. The input saturation is constrained by $\|u_i\|_\infty \le \bar{u}_i$, where the bound $\bar{u}_i$ is assumed to be known.

The dynamical model of the virtual leader is formulated as follows:

$$\begin{cases} \dot{\eta}(t) = A^\eta \eta(t), \\ y^\eta(t) = C^\eta \eta(t), \end{cases} \tag{2}$$

where $\eta \in \mathbb{R}^{n_\eta}$ is the state vector of the virtual leader, $y^\eta \in \mathbb{R}^\eta$ is its output representing the motion trajectory, and A^η and C^η are its state and output matrices, respectively. Similarly, the TVF for each agent, which specifies its desired relative displacement from the leader, is modeled by its own dynamics:

$$\begin{cases} \dot{f}_i(t) = A_i^f f_i(t), \\ y_i^f(t) = C_i^f f_i(t), \end{cases} \tag{3}$$

where $f_i \in \mathbb{R}^{n_{f_i}}$ is the state of the i-th TVF, and $y_i^f \in \mathbb{R}^{p_i}$ is its output. The matrices A_i^f and C_i^f are the corresponding state and output matrices for each agent $i \in \mathcal{M}$.

B. Theoretical Foundations

To ensure the proposed control framework is well-posed, foundational conditions are required. Additionally, formally guaranteeing collision-free physical safety demands a rigorous mathematical tool. The following assumptions and definitions lay these prerequisites.

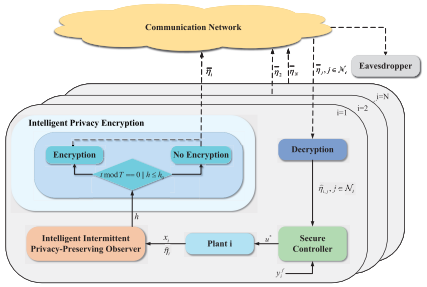

Fig. 1. Dual-layer control architecture for privacy-preserving state estimation and secure control.

Assumption 1: The system matrices, A^η and A_i^f for all $i \in \mathcal{M}$, have no eigenvalues with positive real parts. The pair (A_i, B_i) is controllable.

Assumption 2 ([18]): For every $\lambda \in \sigma(A_i^\zeta)$,

$$\operatorname{rank}\begin{bmatrix} A_i - \lambda I_{n_i} & B_i \\ C_i & 0 \end{bmatrix} = n_i + p, \quad i = 1, 2, \ldots, n$$

where $A_i^\zeta = \begin{pmatrix} A^\eta & 0 \\ 0 & A_i^f \end{pmatrix}$, and $\sigma(A_i^\zeta)$ denotes the spectrum of A_i^ζ.

Assumption 3 ([16]): The communication graph of the HMAS contains a spanning tree rooted at the virtual leader, and the subgraph formed by the remaining agents is connected.

Assumption 4: The static and dynamic obstacles in the workspace are assumed to be sufficiently sparse such that, for each agent, there exists at least one admissible control input satisfying all ECBF constraints and the input saturation limits.

Definition 1 ([37]): Let $h : D \to \mathbb{R}$ be a r^b-times continuously differentiable function defined on a domain $D \subset \mathbb{R}^n$. Define the superlevel set

$$\mathcal{C} := \{x \in D \mid h(x) \ge 0\}, \quad \operatorname{Int}(\mathcal{C}) := \{x \in D \mid h(x) > 0\}.$$

The function $h(x)$ is said to be the safety constraint function of relative degree $r^b \in \mathbb{N}$ if there exists a row vector $K_h^\alpha \in \mathbb{R}^{r^b}$ such that for all $x \in \operatorname{Int}(\mathcal{C})$,

$$\sup_{u \in U} h^{(r^b)}(x, u) \ge -K_h^\alpha v_b^h(x), \tag{4}$$

and if the initial condition satisfies $h(x_0) \ge 0$, then the following inequality holds for all $t \ge 0$:

$$h(x(t)) \ge C e^{(F - G K_h^\alpha)t} v_b^h(x_0) \ge 0 \tag{5}$$

where $h^{(r^b)}(x, u)$ denotes the r^b-th time derivative of $h(x)$ along the system trajectory, $v_b^h(x)$ collects the Lie derivatives of $h(x)$ up to order $r^b - 1$, and F, G, and C are the linear system state, input, and output matrices of the system.

This article focuses on addressing the following problem. The safe TVF control problem aims to design a resilient observer and a controller for the system as described in (2) under input saturation, ensuring that as follows:

1) Ensure the TVF error $\lim_{t\to\infty} \|e_i(t)\|$ is bounded for $i \in \mathcal{M}$, where $e_i(t) = y_i(t) - y^\eta(t) - y_i^f(t)$.
2) For any $i \in \mathcal{M}$ and $o \in \mathcal{O}_i$, $\|y_i(t) - y_o\| - D_{io} > 0$.

III. Secure Formation Control Strategy

A unified two-layer framework for secure TVF control is proposed in Fig. 1.

A. Intelligent Intermittent Privacy-Preserving Observer

$$\delta_j(t) = \begin{cases} \mu_j e^{\frac{r_j}{(T_{2m}-t)(T_{2m+1}-t)}}, & t \in (T_{2m}, T_{2m+1}) \\ 0, & \text{otherwise} \end{cases} \tag{6}$$

where $\mu_j \in \mathbb{R}^{n_\eta}$ is the masking amplitude vector (or $\mu_j > 0$ can be a scalar if applied uniformly and $r_j > 0$ controls the sharpness of the perturbation profile. This function ensures that the mask will appear and vanish smoothly at the boundaries of each activation interval:

$$\lim_{t \to T_{2m}^+} \delta_j(t) = \mathbf{0}, \quad \lim_{t \to T_{2m+1}^-} \delta_j(t) = \mathbf{0}.$$

Furthermore, the mask $\delta_j(t)$ is bounded, i.e., $\|\delta_j(t)\| \le \|\mu_j\|$ for $t \in (T_{2m}, T_{2m+1})$, and $\delta_j(t) = \mathbf{0}$ outside these intervals.

In light of the fact that not all agents can directly access the virtual leader, a distributed linear observer is designed to allow each agent to estimate the leader's state based solely on local information exchange. The observer for agent $i \in \mathcal{M}$ is given by

$$\dot{\hat{\eta}}_i(t) = A^\eta \hat{\eta}_i(t) - k\xi_i(t) \tag{7}$$

$$\xi_i(t) = \sum_{j=0}^{n} a_{ij}(\hat{\eta}_i(t) - \hat{\eta}_j(t)) \tag{8}$$

where $\hat{\eta}_i$ is the estimated state of the virtual leader by agent i, η is the true state of the virtual leader with $\hat{\eta}_0 = \eta$, $k > 0$ is the observer gain, and a_{ij} are elements representing the communication link from agent j to agent i. The estimation error is defined as $\tilde{\eta}_i = \eta - \hat{\eta}_i$.

Each follower agent $j \in \mathcal{M}$ masks its state estimate $\hat{\eta}_j(t)$ before transmission, while the virtual leader, designated as agent 0, masks its true state $\eta(t)$. The signal transmitted by agent j is given by

$$\bar{\eta}_j(t) = \hat{\eta}_j(t) + \delta_j(t) \tag{9}$$

where $\delta_j(t) \in \mathbb{R}^{n_\eta}$ is the intermittent masking signal as defined in (6). To mitigate the interference of masking on state estimation without relying on additional communication overhead, an explicit decryption layer is introduced at the receiver, with the decryption operation relying on a locally constructed signal $\delta_i'(t)$. The core design of $\delta_i'(t)$ lies in its consistent masking mechanism with the sender's $\delta_j(t)$. During periodic IPP intervals, $\delta_i'(t)$ is set as the masking signal locally generated by receiver i $\delta_i'(t) = \delta_i(t))$, enabling the receiver to attenuate the sender's masking effect through the operation $\bar{\eta}_j(t) - \delta_i'(t)$. This attenuation reduces the masking-induced distortion to a bounded range that the observer can tolerate, balancing privacy protection and estimation performance. Outside periodic IPP intervals, no decryption operation is required, $\delta_i'(t)$is set to a zero vector. The dynamics of the observer in (9) are designed as follows:

$$\dot{\hat{\eta}}_i(t) = A^\eta \hat{\eta}_i(t) - k \sum_{j=0}^{n} a_{ij}(\hat{\eta}_i(t) - \hat{\eta}_{i,j}(t)). \tag{10}$$

where $\hat{\eta}_{i,j}(t) = \bar{\eta}_j(t) - \delta_i'(t)$.

Remark 1: (6) employs a smooth bump function to satisfy the differentiability requirements imposed by the UAVs' relative degree of 4, which prevents control input spikes and actuator saturation.

B. Secure Controller For Safe Time-Varying Formation

For safe TVF control, the multi-target tracking problem is simplified by augmenting the reference dynamics into a single system, combining the virtual leader and n TVF trajectories. A physical-layer secure controller is constructed, by which cooperative tracking of the augmented reference is guaranteed while all physical constraints are respected. The dynamics of this augmented system can be written as

$$\dot{\zeta}_i(t) = A_i^\zeta \zeta_i(t) \tag{11}$$

$$y_i^\zeta(t) = C_i^\zeta f_i(t) \tag{12}$$

where $A_i^\zeta = \begin{pmatrix} A^\eta & 0 \\ 0 & A_i^f \end{pmatrix}$ is the augmented state matrix formed by the block diagonal of the leader and TVF state matrices, $C_i^\zeta = [C^\eta, C_i^f]$ is the augmented output matrix, and $\zeta_i = \mathrm{col}(\eta, f_i)$ represents the i-th reference system's augmented state vector, with its dimension given by $n_{\zeta_i} = n_\eta + n_f$. The TVF error is defined as $e_i(t) = y_i(t) - y^\eta(t) - y_i^f(t) = y_i(t) - C_i^\zeta \zeta_i(t), \quad i = 0, 1, \ldots, n$. Under the observer (10), the estimated reference state is $\hat{\zeta}_i(t) = \mathrm{col}(\hat{\eta}_i(t), f_i(t))$ and the estimation error $\tilde{\zeta}_i(t) = \zeta_i(t) - \hat{\zeta}_i(t)$ is also bounded.

According to the internal model principle [38], the augmented MAS can be constructed as

$$\dot{x}_i(t) = A_i x_i(t) + B_i u_i(t), \ i \in \mathcal{M} \tag{13}$$

$$\dot{z}_i(t) = \Phi_{i1} z_i(t) + \Phi_{i2} \hat{e}_i(t) \tag{14}$$

$$\hat{e}_i(t) = y_i - C_i^\zeta \hat{\zeta}_i(t) \tag{15}$$

where z_i is the internal compensation state and (Φ_{i1}, Φ_{i2}) is the p-copy internal model pair of A_i^ζ.

Define the augmented state $\chi_i = \mathrm{col}(x_i, z_i)$, then the overall dynamics become:

$$\dot{\chi}_i(t) = A_i^\chi \chi_i(t) + B_i^\chi u_i(t) + B_i^\zeta \hat{\zeta}_i(t), \tag{16}$$

$$\hat{e}_i(t) = C_i^\chi \chi_i(t) - C_i^\zeta \hat{\zeta}_i(t), \tag{17}$$

with the matrices defined as $A_i^\chi = \begin{bmatrix} A_i & 0 \\ \Phi_{i2} C_i & \Phi_{i1} \end{bmatrix}, B_i^\chi = \begin{bmatrix} B_i \\ 0 \end{bmatrix}, B_i^\zeta = \begin{bmatrix} 0 \\ -\Phi_{i2} C_i^\zeta \end{bmatrix}, C_i^\chi = \begin{bmatrix} C_i & 0 \end{bmatrix}$.

A state error associated with the output error is defned as

$$\tilde{\chi}_i = \chi_i - \Pi_i^\zeta \hat{\zeta}_i \tag{18}$$

where $\Pi_i^\zeta = \mathrm{col}(\Pi_i^\chi, \Pi_i^z)$ and U_i^ζ are a pair of solutions [39] that satisfy the following output regulation equations:

$$\Pi_i^\chi A_i^\zeta = A_i \Pi_i^\chi + B_i U_i^\zeta \tag{19}$$

$$\Pi_i^z A_i^\zeta = \Phi_{i1} \Pi_i^z + \Phi_{i2}(C_i \Pi_i^\chi - C_i^\zeta) \tag{20}$$

$$C_i \Pi_{i1}^\zeta - C_i^\zeta = 0. \tag{21}$$

To ensure safety against obstacles while respecting input saturation, the distinct dynamics of the heterogeneous agents must be modeled. The HMAS consists of UAVs (set $\mathcal{M}_1$) and

UGVs (set $\mathcal{M}_2$), where $\mathcal{M}_1 \cup \mathcal{M}_2 = \mathcal{M}$. Each agent $i \in \mathcal{M}$ has position $p_i = \mathrm{col}(p_i^x, p_i^y)$, velocity $v_i = \mathrm{col}(v_i^x, v_i^y)$.

For $i \in \mathcal{M}_1$, the state vector is $x_i = \mathrm{col}(p_i, v_i, \theta_i, q_i) \in \mathbb{R}^8$. The system matrices are:

$$A_i = \begin{bmatrix} 0 & I & 0 & 0 \\ 0 & 0 & G & 0 \\ 0 & 0 & 0 & I \\ 0 & 0 & 0 & 0 \end{bmatrix}, \quad B_i = \begin{bmatrix} 0 \\ 0 \\ 0 \\ F \end{bmatrix}, \quad C_i = \begin{bmatrix} I & 0 & 0 & 0 \end{bmatrix}. \tag{22}$$

where the attitude is represented by pitch and roll angles $\theta_i = \mathrm{col}(\theta_i^x, \theta_i^y)$ and corresponding angular rates $q_i = \mathrm{col}(q_i^x, q_i^y)$. The UAV acceleration model includes gravity $G = \mathrm{diag}(g, -g)$, and a torque input mapping $F = \mathrm{diag}(k_i^m L_i / I_i^x, k_i^m L_i / I_i^y)$, where g is gravitational acceleration, k_i^m is the force coefficient, L_i is the arm length, I_i^x, I_i^y are the moments of inertia in the x and y directions. The UAVs are assumed to fly within a fixed horizontal plane. This plane is safely above the UGVs, so we focus on their 2D motion and only consider potential collisions: among UAVs, among UGVs and with obstacles in the same horizontal plane.

For $i \in \mathcal{M}_1$, we define the colliding set within its detection range as $\mathcal{O}_i$, which includes both static and dynamic obstacles.

For each $j \in \mathcal{O}_i \cap \mathcal{M}_1$, the safety constraint is given as

$$h_{ij} = (p_i - p_j)^{\mathrm{T}}(p_i - p_j) - D_{ij}^{\mathrm{T}} D_{ij} \tag{23}$$

where D_{ij} is the safe distance between agents i and j. It defines a safe set $S_{ij} = \{h_{ij} \geq 0\}$. The safety constraint is

$$h_{ij}^{(4)} \geq -K_{h_{ij}}^{\alpha} H_{ij} \tag{24}$$

where $H_{ij} = \left[h_{ij}^{\mathrm{T}}, \dot{h}_{ij}^{\mathrm{T}}, \ddot{h}_{ij}^{\mathrm{T}}, (h_{ij}^{(3)})^{\mathrm{T}}\right]^{\mathrm{T}}$, with $\dot{h}_{ij} = 2(p_i - p_j)^{\mathrm{T}}(v_i - v_j)$, $\ddot{h}_{ij} = 2(v_i - v_j)^{\mathrm{T}}(v_i - v_j) + 2(p_i - p_j)^{\mathrm{T}} G(\theta_i - \theta_j)$, $h_{ij}^{(3)} = 6(v_i - v_j)^{\mathrm{T}} G(\theta_i - \theta_j) + 2(p_i - p_j)^{\mathrm{T}} G(q_i - q_j)$, and $h_{ij}^{(4)} = 6(G(\theta_i - \theta_j))^{\mathrm{T}} G(\theta_i - \theta_j) + 8(v_i - v_j)^{\mathrm{T}} G(q_i - q_j) + 2(p_i - p_j)^{\mathrm{T}} G F(u_i - u_j)$.

Then, safety constraint (24) can be rewritten as

$$-A_{ij}^h (u_i - u_j) \leq b_{ij}^h \quad \forall j \in \mathcal{O}_i \cap \mathcal{M}_1 \tag{25}$$

where $A_{ij}^h = 2(p_i - p_j)^{\mathrm{T}} G F$ and $b_{ij}^h = 6(G(\theta_i - \theta_j))^{\mathrm{T}} G(\theta_i - \theta_j) + 8(v_i - v_j)^{\mathrm{T}} G(q_i - q_j) + K_{h_{ij}}^{\alpha} H_{ij}$.

Inspired by the decoupling method in [40], decoupling parameters d_{ij} based on agent input saturation are introduced to partition the condition of (25) into the following two conditions:

$$-A_{ij}^h u_i \leq d_{ij} b_{ij}^s \tag{26}$$

$$-A_{ji}^h u_j \leq d_{ji} b_{ji}^s \tag{27}$$

where $d_{ij} = \frac{\bar{u}_i}{\bar{u}_i + \bar{u}_j}$ and $d_{ij} + d_{ji} = 1$. Assuming $A_{ij}^h = -A_{ji}^h$ and $K_{h_{ij}}^{\alpha} = K_{h_{ji}}^{\alpha}$, it follows that $b_{ij}^h = b_{ji}^h$.

For obstacles $k \in \mathcal{O}_i \setminus \mathcal{M}_1$, the safety constraint is

$$h_{ik} = (p_i - p_k)^{\mathrm{T}}(p_i - p_k) - d_{ik}^{\mathrm{T}} d_{ik} \tag{28}$$

with safety constraint:

$$-A_{ik}^h u_i \leq b_{ik}^h \quad \forall k \in \mathcal{O}_i \setminus \mathcal{M}_1 \tag{29}$$

where the coefficient matrix is defined as $A_{ik}^h = 2(p_i - p_k)^{\mathrm{T}} G F$, and the bound b_{ik}^h is computed as $b_{ik}^h = 6(G\theta_i)^{\mathrm{T}} G\theta_i + 8\, v_i^{\mathrm{T}} G q_i + K_{h_{ik}}^{\alpha} H_{ik}$.

Here, $H_{ik} = \left[h_{ik}, \dot{h}_{ik}, \ddot{h}_{ik}, h_{ik}^{(3)}\right]^{\mathrm{T}}$ contains the derivatives of the safety constraint, where $\dot{h}_{ik} = 2(p_i - p_k)^{\mathrm{T}} v_i$, $\ddot{h}_{ik} = 2\, v_i^{\mathrm{T}} v_i + 2(p_i - p_k)^{\mathrm{T}} G\theta_i$, and $h_{ik}^{(3)} = 6\, v_i^{\mathrm{T}} G\theta_i + 2(p_i - p_k)^{\mathrm{T}} G q_i$.

For $i \in \mathcal{M}_2$, the UGV dynamics is a second-order system with state $x_i = \mathrm{col}(p_i, v_i) \in \mathbb{R}^4$ and system matrices given as follows:

$$A_i = \begin{bmatrix} 0 & I \\ 0 & 0 \end{bmatrix}, \quad B_i = \begin{bmatrix} 0 \\ I \end{bmatrix}, \quad C_i = \begin{bmatrix} I & 0 \end{bmatrix}, \tag{30}$$

Following the same ECBF construction procedure as that for UAVs, the pairwise safety function between agents i and j is defined as

$$h_{ij} = (p_i - p_j)^{\mathrm{T}}(p_i - p_j) - D_{ij}^{\mathrm{T}} D_{ij}. \tag{31}$$

Since the UGV model has relative degree two with respect to h_{ij}, the safety condition is enforced by a second-order ECBF

$$h_{ij}^{(2)} \geq -K_{h_{ij}}^{\alpha} H_{ij}, \tag{32}$$

where $H_{ij} = [h_{ij}, \dot{h}_{ij}]^{\mathrm{T}}$.

After straightforward differentiation, the constraint can be written in an affine form with respect to the control inputs as

$$-A_{ij}^{\ell}(u_i - u_j) \leq b_{ij}^{\ell}, \quad \forall j \in \mathcal{O}_i \cap \mathcal{M}_2, \tag{33}$$

where $A_{ij}^{\ell} = 2(p_i - p_j)^{\mathrm{T}}$ and b_{ij}^{ℓ} collects the remaining state-dependent terms.

To enable distributed implementation under input saturation, the above coupled constraint is decoupled using the same strategy as in the UAV case, yielding

$$-A_{ij}^{\ell} u_i \leq d_{ij} b_{ij}^{\ell}, \qquad -A_{ji}^{\ell} u_j \leq d_{ji} b_{ji}^{\ell}, \tag{34}$$

with $d_{ij} = \bar{u}_i / (\bar{u}_i + \bar{u}_j)$ and $d_{ij} + d_{ji} = 1$.

For static obstacles $k \in \mathcal{O}_i \setminus \mathcal{M}_2$, the safety constraint admits the same affine form

$$-A_{ik}^{\ell} u_i \leq b_{ik}^{\ell}, \tag{35}$$

where $A_{ik}^{\ell} = 2(p_i - p_k)^{\mathrm{T}}$ and b_{ik}^{ℓ} is defined accordingly.

IV. Main Results

This section establishes the stability properties of the proposed framework. Specifically, Theorem 1 proves the uniform ultimate boundedness of the observer estimation error, while Theorem 2 guarantees that the secure controller achieves ultimately bounded formation tracking under all safety and input constraints.

To this end, define the stacked observer error $\tilde{\eta} = \mathrm{col}(\tilde{\eta}_1, \ldots, \tilde{\eta}_n)$ for all n followers. The communication topology of the leader–follower network is characterized by the Laplacian matrix

$$L_{n+1} = \begin{bmatrix} 0 & 0_{1\times n} \\ L_0 & L_1 \end{bmatrix}, \tag{36}$$

where $L_1 \in \mathbb{R}^{n\times n}$ describes the inter-follower connectivity and $L_0 \in \mathbb{R}^{n\times 1}$ represents the leader–follower coupling.

Considering the decoding mismatch caused by asynchronous triggering or communication jitter, we model the received state as:

$$\hat{\eta}_{i,j}(t) = \hat{\eta}_j(t) + \Delta\delta_{ij}(t) \tag{37}$$

where $\Delta\delta_{ij}(t) = \delta_j(t) - \delta'_j(t)$ is defined as the residual mask error, $\|\Delta\delta_{ij}\| \le \delta_{max}$. Using (2), (3) and (9), we have

$$\begin{aligned}\dot{\tilde{\eta}}_i &= A^{\eta}\tilde{\eta}_i + k\sum_{j=0}^{n} a_{ij}(\tilde{\eta}_i - \tilde{\eta}_j + \Delta\delta_{ij}(t)) \\ &= A^{\eta}\tilde{\eta}_i + k\sum_{j=0}^{n} a_{ij}(\tilde{\eta}_i - \tilde{\eta}_j) + w_i(t)\end{aligned} \tag{38}$$

where $\tilde{\eta}_0(t) = \mathbf{0}$, $w_i(t) = k\sum_{j=0}^{n} a_{ij}\Delta\delta_{ij}(t)$. Therefore, the global error dynamics equation can be written as

$$\dot{\tilde{\eta}} = (I_n \otimes A^{\eta} - k(L_1 \otimes I_{n_\eta}))\tilde{\eta} + w(t)$$

where $w(t)$ is the stacked vector of all node disturbance terms.

Then, the following theorem demonstrates the uniform ultimate boundedness of the observation error.

Theorem 1: Given that Assumptions 1 to 3 hold and the intelligent intermittent privacy-preserving mechanism is adopted, for the HMAS (2), (3), the estimation error of the designed observer (10) is uniformly ultimately bounded.

Proof: Since the observation vector $\tilde{\eta}$ cannot be measured directly, we construct an auxiliary variable:

$$\xi = (L_f \otimes I_{n_\eta})\tilde{\eta}. \tag{39}$$

where $L_f \otimes I_{n_\eta} = I_n \otimes A^{\eta} - k(L_1 \otimes I_{n_\eta})$.

Differentiating with respect to ξ, we obtain the dynamic equation with a disturbance term:

$$\dot{\xi} = H\xi + \Psi w(t) \tag{40}$$

where $H = (I_n \otimes A^{\eta} - k(L_1 \otimes I_{n_\eta}))$, $\Psi = L_f \otimes I_{n_\eta}$.

Since H is Hurwitz, for any symmetric positive definite matrix $Q > 0$, there exists a unique symmetric positive definite matrix $P > 0$ that satisfies the Lyapunov equation:

$$H^{\mathrm{T}}P + PH = -Q. \tag{41}$$

A Lyapunov function is formulated as

$$V(\tilde{\eta}) = \xi^{\mathrm{T}}P\xi \tag{42}$$

where $P = P^{\mathrm{T}} > 0$. Then we have

$$\begin{aligned}[b]\dot{V} &= \dot{\xi}^T P\xi + \xi^T P\dot{\xi} \\ &= (H\xi + \Psi w)^T P\xi + \xi^T P(H\xi + \Psi w) \\ &= -\xi^T Q\xi + 2\xi^T P\Psi w(t).\end{aligned} \tag{43}$$

Given that the exponential masking function (6) proposed is smooth and satisfies the Lipschitz condition, the disturbance term caused by a bounded time synchronization error τ is also bounded, it satisfies $\|w(t)\| \le w_{\max}$. Using the standard inequality scaling technique, we have

$$\dot{V} \le -\lambda_{\min}(Q)\|\xi\|^2 + 2\|P\|\|\Psi\|w_{\max}\|\xi\|.$$

Thus, as long as the estimation error satisfies $\|\xi\| > \frac{2\|P\|\|\Psi\|w_{\max}}{\lambda_{\min}(Q)} \triangleq \Delta_\eta$, which can be guaranteed that $\dot{V} < 0$. Therefore, it can be concluded that the error variable $\xi(t)$ is uniformly ultimately bounded and exponentially converges to the compact set $\mathcal{D} = \{\xi : \|\xi\| \le \Delta_\eta\}$.

Theorem 2: For the HMAS defined in (22) and (30), the safety constraint functions in (23) and (28) are designed to mitigate collision risks among agents and with environmental obstacles. The system's safe TVF control problem can thus be solved via the observer (10) and the following secure controller:

$$u_i^* = \operatorname{argmin}\ w_1\|u_i\|^2 + w_2\delta_\chi^2 \tag{44}$$

$$\begin{aligned}&2\tilde{\chi}_i^{\mathrm{T}}P_iB_i^{\chi}u_i \le -\tilde{\chi}_i^{\mathrm{T}}\left(P_iA_i^{\chi} + (A_i^{\chi})^{\mathrm{T}}P_i + \beta_\chi P_i\right)\tilde{\chi}_i \\ &\quad - 2\hat{\chi}_iP_iB_i^{\chi}\tilde{\zeta}_i + \delta_\chi, \quad \beta_\chi > 0\end{aligned} \tag{44a}$$

$$\text{if } i \in \mathcal{M}_1, \quad -A_{ij}^h u_i \le d_{ij}b_{ij}^h, -A_{ik}^h u_i \le b_{ik}^h \tag{44b}$$

$$\text{if } i \in \mathcal{M}_2, \quad -A_{ij}^l u_i \le d_{ij}b_{ij}^l, -A_{ik}^l u_i \le b_{ik}^l \tag{44c}$$

$$\|u_i\|_\infty \le \overline{u}_i \tag{44d}$$

where δ_χ is a slack, and $d_{ij} = (\overline{u}_i / [\overline{u}_i + \overline{u}_j])$ is the decoupling parameter. The weight parameters w_1 and w_2 are all positive. If (44) have feasible solutions when $\delta_\chi = 0$ and $\xi \to 0$, then the formation error converges to 0 as time $t \to \infty$.

Proof: Let $V_i^{\chi} = \tilde{\chi}_i^{\mathrm{T}}P_i\tilde{\chi}_i$ be the Lyapunov function, we have

$$\dot{V}_i^{\chi} = \tilde{\chi}_i^{\mathrm{T}}(P_iA_i^{\chi} + (A_i^{\chi})^{\mathrm{T}}P_i) + 2\tilde{\chi}_i^{\mathrm{T}}P_iB_i^{\chi}u_i + 2\tilde{\chi}_i^{\mathrm{T}}P_iB_i^{\zeta}\hat{\zeta}_i. \tag{45}$$

If the inequality (44a) is satisfied, then we have the following condition met:

$$\dot{V}_i^{\chi} + \beta_\chi V_i^{\chi} < \delta_\chi \tag{46}$$

where δ_χ is a non-negative slack variable. We have the state error $\tilde{\chi}_i$ is bounded by

$$\limsup_{t\to\infty}\|\tilde{\chi}_i\|^2 \le \frac{\delta_\chi}{\beta_\chi\lambda_{\min}(P_i)}. \tag{47}$$

Based on the output regulation (24), (25) and (26), we have

$$\hat{e}_i = C_i^{\chi}\chi_i - C_i^{\chi}\hat{\zeta}_i = C_i^{\chi}\tilde{\chi}_i + (C_i^{\chi}\Pi_i^{\zeta} - C_i^{\zeta})\hat{\zeta}_i = C_i^{\zeta}\tilde{\chi}_i \tag{48}$$

$$e_i = \hat{e}_i + C_i^{\zeta}\tilde{\zeta}_i. \tag{49}$$

Since the observer error $\xi(t)$ is uniformly ultimately bounded under the proposed intermittent privacy-preserving mechanism, it follows that $\tilde{\eta}_i(t)$ and $\tilde{\zeta}_i(t)$ are uniformly ultimately bounded for all $i \in \mathcal{M}$. Moreover, we have

$$\|\tilde{\zeta}_i(t)\|^2 = \|\tilde{\eta}_i(t)\|^2 \le \frac{1}{\lambda_{\min}(L_1^{\mathrm{T}}L_1)}\|\xi(t)\|^2. \tag{50}$$

Substituting this result into the output tracking error (47), the formation error $e_i(t)$ satisfies

$$\limsup_{t\to\infty}\|e_i(t)\|^2 \le \|C_i^{\zeta}\|^2\left(\frac{\delta_\chi}{\beta_\chi\lambda_{\min}(P_i)} + \frac{1}{\lambda_{\min}(L_1^{\mathrm{T}}L_1)}\Delta_\eta^2\right), \tag{51}$$

Therefore, under the proposed controller, the formation tracking error $e_i(t)$ is uniformly ultimately bounded.

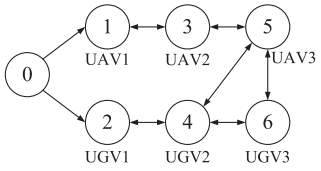

Fig. 2. Communication topology of HMAS.

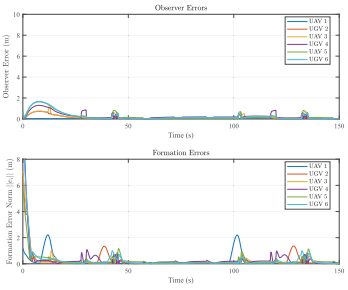

Fig. 3. Observation and formation tracking errors.

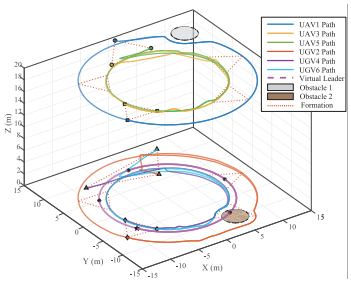

Fig. 4. 3-D trajectories of the Heterogeneous system.

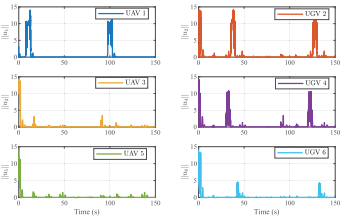

Fig. 5. Control input magnitudes for each agent.

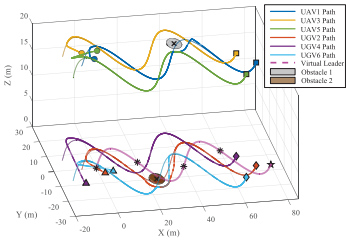

Fig. 6. 3-D trajectories of agents.

V. Simulation Example

To evaluate the proposed framework in heterogeneous systems, representative simulation missions are designed to test formation tracking with respect to a virtual leader and collision-free motion. The desired trajectory is generated by a virtual leader executing a circular motion with angular velocity ω^v, whose state is $v = \mathrm{col}(x_c, y_c, \dot{x}_c, \dot{y}_c)$ and output (x_c, y_c). The circular path is defined by $x_c = b^\eta \sin(\omega^\eta t)$ and $y_c = b^\eta \cos(\omega^\eta t)$, with system matrices

$$A^\eta = \begin{pmatrix} 0 & 1 \\ -\omega^v & 0 \end{pmatrix} \otimes I_2, \quad C^\eta = \begin{pmatrix} 1 & 0 & 0 & 0 \\ 0 & 1 & 0 & 0 \end{pmatrix}. \tag{52}$$

The parameters are set as $b^v = 10$, $\omega^v = 0.07$, and the initial state is $[0, 10, 0.7, 0]^{\mathrm{T}}$.

Both UAVs and UGVs track the virtual leader while orbiting it in different operational layers. The desired relative motion is generated by a time-varying vector field $f_i^x = b_i^f \sin(\omega_i^f t + \theta_i^f)$ and $f_i^y = b_i^f \cos(\omega_i^f t + \theta_i^f)$, where UAV altitude is fixed at H_c and only planar formation is considered. The corresponding TVF system matrices are

$$A_i^f = \begin{bmatrix} 0 & \omega^f \\ -\omega^f & 0 \end{bmatrix}, \quad C_i^f = I_2. \tag{53}$$

The parameters are set as $b^\eta = 3.5$, $\omega^\eta = 0.07$, $\theta_{(1,2)}^f = 0$, $\theta_{(3,4)}^f = \frac{2\pi}{3}$, $\theta_{(5,6)}^f = \frac{4\pi}{3}$, and $H_c = 20$.The communication topology shown in Fig. 2.

The observer and secure controller parameters in (10) and (44) are set as follows: the observer gain is $k = 1.5$, the input saturation limit is $\bar{u}_i = 15$, and the QP weights are chosen as $w_1 = 1$ and $w_2 = 10^3$ to prioritize CLF-based performance. The initial states of the observers and the HMAS are set accordingly. An intelligent intermittent privacy-preserving mechanism is employed, combining a periodic mode and an event-triggered mode activated when $h_0 = 15$, which balances safety warning and control efficiency.

TABLE I

Quantitative Indicators of Privacy Protection Performance (Agent 4)

Metric	Value
Observation window	Step 2500 – Step 7501
Attacker RMSE (m)	1.2177
Legitimate Neighbor RMSE (m)	0.3463
Maximum Attacker Error (m)	1.3559
Privacy Gain (RMSE Ratio)	3.52×

TABLE II

Observation and Formation RMSE Performance Under Different Packet Loss Scenarios

Different Scenarios	Observation RMSE (m)	Formation RMSE (m)
Ideal No Loss	0.1788	0.2909
Regular Low Loss	0.1796	0.2925
Moderate Loss	0.1863	0.2951
Extreme High Loss	0.1882	0.2971

Notes: Packet loss rates (Leader-to-Follower, Follower-to-Follower)
Ideal: (0%, 0%); Low: (1%, 5%); Moderate: (3%, 10%); Extreme: (5%, 15%).

As shown in Fig. 3–6, the observer estimation errors and formation tracking errors converge as guaranteed by Theorems 1 and 2, while all control inputs remain within saturation limits. To evaluate the robustness of the proposed observer and controller under realistic communication conditions, random packet loss is incorporated into the simulation. A Bernoulli packet loss model is adopted to emulate wireless network

TABLE III
QUANTITATIVE TEST RESULTS OF DYNAMIC OBSTACLE AVOIDANCE SCENARIOS

Interaction Scenario	Min. Dist.(m)	Avg. Form. Error(m)
Low-Speed Crossing	4.56	0.5479
Medium-Speed Cut-in	4.26	0.5144
High-Speed Head-on	4.82	0.6198

Notes:Experimental Settings(Obstacle Speed, Obstacle Direction)
Low-Speed: ($v \approx 0.8$ m/s, 90° vertical crossing); Medium-Speed: ($v \approx 1.5$ m/s, acute angle trajectory); High-Speed: ($v \approx 5.0$ m/s, 180° head-on).
Min. Dist.: The absolute minimum Euclidean distance recorded between any agent and the obstacle.

imperfections. As shown in Table II, the proposed observer and controller exhibit favorable robustness across all the considered packet loss scenarios. This indicates that packet loss has a negligible impact on the system performance, which fully verifies the good anti-packet-loss capability of the designed algorithm. Table III validates the controller's adaptability to dynamic threats with varying speeds and directions. The results confirm that the global minimum distance remains strictly safe across all scenarios.

VI. CONCLUSION

This article addresses the critical challenge of integrating information security and physical safety. We propose a unified control framework for reliable operation in complex threats, centered on a cyber-physical architecture: cyber layer uses an IPP observer for confidentiality, physical layer adopts a quadratic programming controller for collision avoidance. Future research will investigate role-aware and risk-aware privacy policies for heterogeneous multi-agent systems. Agents with different operational roles may be assigned differentiated communication schedules. Future work will consider more sophisticated adversarial models, such as attackers with partial prior information or coordinated signal analysis capabilities, and investigate enhanced privacy-preserving mechanisms to further strengthen resilience against advanced eavesdropping attacks.

REFERENCES

[1] S. He, S.-L. Dai, Z. Zhao, T. Zou, and Y. Ma, "UDE-based distributed formation control for MSVs with collision avoidance and connectivity preservation," *IEEE Trans. Ind. Informat.*, vol. 20, no. 2, pp. 1476–1487, Feb. 2024.

[2] W. Xi, M. Hu, H. Wang, H. Dong, and Z. Ying, "Formation control for virtual coupling trains with parametric uncertainty and unknown disturbances," *IEEE Trans. Circuits Syst. II, Exp. Briefs*, vol. 70, no. 9, pp. 3429–3433, Sep. 2023.

[3] L. Zha, J. Miao, J. Liu, E. Tian, and C. Peng, "Neural predictor-based formation control for unmanned surface vehicles under aperiodic DoS attacks: A noncooperative game approach," *IEEE Trans. Veh. Technol.*, vol. 74, no. 10, pp. 15013–15025, Oct. 2025.

[4] Y. Jia, K. Meng, K. Wu, C. Sun, and Z. Y. Dong, "Optimal load frequency control for networked power systems based on distributed economic MPC," *IEEE Trans. Syst., Man, Cybern., Syst.*, vol. 51, no. 4, pp. 2123–2133, Apr. 2021.

[5] Z. Liu, Y. Wu, H. Ge, J. Wang, and Z. Lyu, "Data heterogeneity challenge in consumer electronics: A federated learning solution," *IEEE Trans. Consum. Electron.*, vol. 71, no. 2, pp. 6561–6569, May 2025.

[6] Y. Jia, P. Yong, C. Li, K. Meng, Z. Y. Dong, and C. Sun, "An ADMM-based resilient distributed economic MPC algorithm for frequency restoration and economic dispatch in networked microgrids," *IEEE Trans. Ind. Appl.*, vol. 62, no. 2, pp. 3275–3285, Feb. 2025, doi: 10.1109/TIA.2025.3618824.

[7] V. O. Sivaneri and J. N. Gross, "UGV-to-UAV cooperative ranging for robust navigation in GNSS-challenged environments," *Aerosp. Sci. Technol.*, vol. 71, pp. 245–255, Dec. 2017.

[8] Z. Su, X. Wang, and H. Wang, "Neural-adaptive constrained flight control for air–ground recovery under terrain obstacles," *IEEE Trans. Aerosp. Electron. Syst.*, vol. 58, no. 1, pp. 374–390, Feb. 2022.

[9] G. E. Jan, T. Lei, C.-C. Sun, Z.-Y. You, and C. Luo, "On the problems of drone formation and light shows," *IEEE Trans. Consum. Electron.*, vol. 70, no. 3, pp. 5259–5268, Aug. 2024.

[10] W. Lin, "Intelligent fault diagnosis of consumer electronics sensor in IoE via transformer," *IEEE Trans. Consum. Electron.*, vol. 70, no. 1, pp. 1259–1267, Feb. 2024.

[11] K. Zhang, Y. Zhang, X. Zong, and X. Dong, "Tracking control of heterogeneous multiagent systems with intrinsic nonlinear dynamics in noisy and time-delayed environments," *IEEE Trans. Cybern.*, vol. 55, no. 1, pp. 64–76, Jan. 2025.

[12] D. Meng and J. Zhang, "Cooperative trajectory tracking of heterogeneous networks by distributed learning," *IEEE Trans. Autom. Control*, vol. 70, no. 8, pp. 5397–5412, Aug. 2025.

[13] Y. Jia, F. Luo, J. Bi, Y. Zhang, Z. Y. Dong, and C. Sun, "Physics-data-driven economic model predictive control for wave energy converters," *IEEE Trans. Ind. Informat.*, vol. 21, no. 10, pp. 7774–7783, Oct. 2025.

[14] Y. Sun, B. Yan, P. Shi, and C.-C. Lim, "Consensus for multiagent systems under output constraints and unknown control directions," *IEEE Syst. J.*, vol. 17, no. 1, pp. 1035–1044, Mar. 2023.

[15] B. Yan, P. Shi, and J. Chambers, "Cooperative control for heterogeneous multi-agent systems: Progress, applications, and challenges," *Sci. China Inf. Sci.*, vol. 67, no. 5, May 2024, Art. no. 156201.

[16] B. Yan, P. Shi, C. P. Lim, Y. Sun, and R. K. Agarwal, "Security and safety-critical learning-based collaborative control for multiagent systems," *IEEE Trans. Neural Netw. Learn. Syst.*, vol. 36, no. 2, pp. 2777–2788, Feb. 2025.

[17] L. Xia, Q. Li, R. Song, and Z. Zhang, "Leader-follower time-varying output formation control of heterogeneous systems under cyber attack with active leader," *Inf. Sci.*, vol. 585, pp. 24–40, Jan. 2021.

[18] J. Huang, *Nonlinear Output Regulation: Theory and Applications*. Philadelphia, PA, USA: SIAM, 2004.

[19] Q. Wang, Y. Hua, X. Dong, P. Shu, J. Lü, and Z. Ren, "Finite-time time-varying formation tracking for heterogeneous nonlinear multiagent systems using adaptive output regulation," *IEEE Trans. Cybern.*, vol. 54, no. 4, pp. 2460–2471, Apr. 2024.

[20] S. Shao, J. Zhang, T. Wang, A. Shankar, and C. Maple, "Dynamic obstacle-avoidance algorithm for multi-robot flocking based on improved artificial potential field," *IEEE Trans. Consum. Electron.*, vol. 70, no. 1, pp. 4388–4399, Feb. 2024.

[21] Y. Sun et al., "PPDR: A privacy-preserving dual reputation management scheme in vehicle platoon," *IEEE Trans. Dependable Secure Comput.*, vol. 22, no. 6, pp. 6636–6652, Nov. 2025.

[22] J. Liu, Z. Liu, Y. Li, E. Tian, and C. Peng, "Privacy-protected formation control for unmanned surface vehicles: A neural predictor-based non-cooperative game framework," *IEEE Trans. Veh. Technol.*, early access, Jan. 12, 2026, doi: 10.1109/TVT.2026.3651837.

[23] Z. Chen, Y. Guo, and J. Hao, "Dynamic trajectory design for multi-UAV assisted long-term data collection tasks," *IEEE Trans. Consum. Electron.*, vol. 71, no. 2, pp. 5960–5968, May 2025.

[24] J. Liu, E. Ma, L. Zha, and E. Tian, "Distributed energy management for microgrids: When privacy preservation meets multiple mechanisms," *IEEE Trans. Consum. Electron.*, early access, Jan. 6, 2026, doi: 10.1109/TCE.2026.3651619.

[25] J. Hu, Q. Sun, R. Wang, B. Wang, M. Zhai, and H. Zhang, "Privacy-preserving sliding mode control for voltage restoration of AC microgrids based on output mask approach," *IEEE Trans. Ind. Informat.*, vol. 18, no. 10, pp. 6818–6827, Oct. 2022.

[26] M. Wang, H. Liang, Y. Pan, and X. Xie, "A new privacy preservation mechanism and a gain iterative disturbance observer for multiagent systems," *IEEE Trans. Netw. Sci. Eng.*, vol. 11, no. 1, pp. 392–403, Jan. 2024.

[27] S. Yang, H. Liang, Y. Pan, and T. Li, "Security control for air-sea heterogeneous multiagent systems with cooperative-antagonistic interactions: An intermittent privacy preservation mechanism," *Sci. China Technological Sci.*, vol. 68, no. 4, Apr. 2025, Art. no. 1420402.

[28] H. Yang, Y. He, Y. Xu, and H. Zhao, "Collision avoidance for autonomous vehicles based on MPC with adaptive APF," *IEEE Trans. Intell. Vehicles*, vol. 9, no. 1, pp. 1559–1570, Jan. 2024.

[29] C. Mu, J. Yao, H. Yang, M. Lu, and Q. Han, "Cooperative control for air-ground systems via bidirectional signal connection in complex environment," *IEEE Trans. Syst., Man, Cybern., Syst.*, vol. 54, no. 9, pp. 5680–5691, Sep. 2024.
[30] L. Zha, J. Miao, J. Liu, E. Tian, and C. Peng, "Data-driven decentralized resilient control for large-scale systems under DoS attacks," *IEEE Trans. Consum. Electron.*, vol. 71, no. 2, pp. 5310–5320, May 2025.
[31] Y. Jia, Z. Y. Dong, C. Sun, and K. Meng, "A tube-based distributed MPC based method for low-carbon energy networks with exogenous disturbances," *IEEE Trans. Netw. Sci. Eng.*, vol. 12, no. 1, pp. 381–391, Jan. 2025.
[32] L. Wang, A. D. Ames, and M. Egerstedt, "Safety barrier certificates for collisions-free multirobot systems," *IEEE Trans. Robot.*, vol. 33, no. 3, pp. 661–674, Jun. 2017.
[33] T. G. Molnar, A. K. Kiss, A. D. Ames, and G. Orosz, "Safety-critical control with input delay in dynamic environment," *IEEE Trans. Control Syst. Technol.*, vol. 31, no. 4, pp. 1507–1520, Jul. 2023.
[34] B. Yan, J. Ni, Y. Zhong, D. Yu, and Z. Wang, "Collision-free formation control for heterogeneous multiagent systems under DoS attacks," *IEEE Trans. Cybern.*, vol. 54, no. 10, pp. 6244–6255, Oct. 2024.
[35] C. Lei, J. Zhang, H. Chen, H. Zhao, L. Zhou, and X. Zhang, "Cooperative optimization on computation, communication and trajectory for UAV crowdsensing: A multi-agent deep reinforcement learning approach," *IEEE Trans. Consum. Electron.*, vol. 71, no. 4, pp. 10837–10852, Nov. 2025.
[36] M. Xi et al., "High-precision underwater perception and path planning of AUVs based on quantum-enhanced," *IEEE Trans. Consum. Electron.*, vol. 70, no. 3, pp. 5607–5617, Aug. 2024.
[37] H. Dai, L. Ji, X. Guo, C. Zhang, S. Yang, and H. Li, "Leader-following synchronization control of multiagent systems under hybrid cyber attacks via impulsive control based on topology switching," *IEEE Trans. Cybern.*, vol. 54, no. 9, pp. 5297–5308, Sep. 2024.
[38] W. Cheng, K. Zhang, B. Jiang, and S. Simani, "Neural network observer-based prescribed-time fault-tolerant tracking control for heterogeneous multiagent systems with a leader of unknown disturbances," *IEEE Trans. Aerosp. Electron. Syst.*, vol. 59, no. 6, pp. 9042–9053, Dec. 2023.
[39] S. Zuo, Y. Song, F. L. Lewis, and A. Davoudi, "Output containment control of linear heterogeneous multi-agent systems using internal model principle," *IEEE Trans. Cybern.*, vol. 47, no. 8, pp. 2099–2109, Aug. 2017.
[40] J. Liu, Y. Dong, L. Zha, X. Xie, and E. Tian, "Reinforcement learning-based tracking control for networked control systems with DoS attacks," *IEEE Trans. Inf. Forensics Security*, vol. 19, pp. 4188–4197, 2024.

Jinliang Liu (Senior Member, IEEE) received the Ph.D. degree in control theory and control engineering from Donghua University, Shanghai, China, in 2011. He was a Lecturer from June 2011 to August 2013, an Associate Professor from August 2013 to July 2019, and a Professor from July 2019 to May 2023 with the School of Information Engineering, Nanjing University of Finance and Economics. He held a Post-Doctoral Position with the School of Automation, Southeast University, Nanjing, China, from December 2013 to June 2016. He was a Visiting Researcher/Scholar with the Department of Mechanical Engineering, The University of Hong Kong from October 2016 to October 2017, and a Visiting Scholar with the Department of Electrical Engineering, Yeungnam University, Gyeongsan, South Korea, from November 2017 to January 2018. Since June, 2023, he has been a Professor with the School of Computer Science, Nanjing University of Information Science and Technology, Nanjing, China. His research interests include cyber-physical systems, autonomous systems, privacy preservation, and game theory.

Shiming Mao received the B.S. degree in computer science and technology from Nanjing University of Information Science and Technology in 2024, where she is currently pursuing the M.S. degree with the School of Computer and Software and the School of Cybersecurity. Her research interests include formation control, robust control, and multiagent systems.

Lijuan Zha received the Ph.D. degree in control science and engineering from Donghua University, Shanghai, China, in 2018. From 2018 to 2024, she was a Lecturer and then an Associate Professor with the College of Information Engineering, Nanjing University of Finance and Economics. In 2024, she joined the Nanjing Forestry University, Nanjing, where she is currently a Professor with the College of Science. From 2018 to 2023, she was a Post-Doctoral Research Associate with the School of Mathematics, Southeast University, Nanjing. Her current research interests include networked control systems, neural networks, complex dynamical systems and multi-agent systems.

Engang Tian (Senior Member, IEEE) received the B.S. degree in mathematics from Shandong Normal University, Jinan, China, in 2002, the M.Sc. degree in operations research and cybernetics from Nanjing Normal University, Nanjing, China, in 2005, and the Ph.D. degree in control theory and control engineering from Donghua University, Shanghai, China, in 2008. From 2011 to 2012, he was a Post-Doctoral Research Fellow with The Hong Kong Polytechnic University. From 2008 to 2018, he was an Associate Professor and later a Professor with the School of Electrical and Automation Engineering, Nanjing Normal University. In 2018, he joined University of Shanghai for Science and Technology, where he is currently a Professor with the School of Optical-Electrical and Computer Engineering. His research interests include networked control systems, cyber attack, and nonlinear stochastic control and filtering.

Chen Peng (Senior Member, IEEE) received the B.S. and M.S. degrees in coal preparation, and the Ph.D. degree in control theory and control engineering from the Chinese University of Mining and Technology, Xuzhou, China, in 1996, 1999, and 2002, respectively. From September 2002 to August 2004, he was a Post-Doctoral Research Fellow in applied mathematics with Nanjing Normal University, China. From November 2004 to January 2005, he was a Research Associate with The University of Hong Kong. From September 2010 to August 2012, he was a Post-Doctoral Research Fellow with Central Queensland University, Australia. He is currently a Professor with the School of Mechatronic Engineering and Automation, Shanghai University. His research interests include networked control systems, multiagent systems, power systems and interconnected systems.